Dalton Transactions

ROYAL SOCIETY OF CHEMISTRY

PAPER

View Article Online
View Journal | View Issue

Cite this: *Dalton Trans.*, 2020, **49**, 511

Towards dual SPECT/optical bioimaging with a mitochondrial targeting, ^{99m}Tc(I) radiolabelled 1,8-naphthalimide conjugate†

Adam H. Day,[a] Juozas Domarkas,[b] Shubhanchi Nigam,[b] Isaline Renard,[b] Christopher Cawthorne,[b] Benjamin P. Burke,[b] Gurmit S. Bahra,[c] Petra C. F. Oyston,[c] Ian A. Fallis,*[a] Stephen J. Archibald*[b] and Simon J. A. Pope*[a]

A series of six different 1,8-naphthalimide conjugated dipicolylamine ligands (**L$^{1-6}$**) have been synthesised and characterised. The ligands possess a range of different linker units between the napthalimide fluorophore and dipcolylamine chelator which allow the overall lipophilicity to be tuned. A corresponding series of Re(I) complexes have been synthesised of the form *fac*-[Re(CO)$_3$(**L$^{1-6}$**)]BF$_4$. The absorption and luminescence properties of the ligands and Re(I) complexes were dominated by the intramolecular charge transfer character of the substituted fluorophore (typically absorption *ca.* 425 nm and emission *ca.* 520 nm). Photophysical assessments show that some of the variants are moderately bright. Radiolabelling experiments using a water soluble ligand variant (**L^5**) were successfully undertaken and optimised with *fac*-[^{99m}Tc(CO)$_3$(H$_2$O)$_3$]$^+$. Confocal fluorescence microscopy showed that *fac*-[Re(CO)$_3$(**L^5**)]$^+$ localises in the mitochondria of MCF-7 cells. SPECT/CT imaging experiments on naïve mice showed that *fac*-[^{99m}Tc(CO)$_3$(**L^5**)]$^+$ has a relatively high stability *in vivo* but did not show any cardiac uptake, demonstrating rapid clearance, predominantly *via* the biliary system along with a moderate amount cleared renally.

Received 14th October 2019,
Accepted 9th December 2019

DOI: 10.1039/c9dt04024b

rsc.li/dalton

Introduction

The different bioimaging modalities each have intrinsic strengths and weaknesses, with no single clinically used technique providing comprehensive information. Prospective multimodal imaging agents are designed to combine the strengths of individual modalities, while offering complementary or additional clinically useful information not provided by a single technique.[1,2] Single photon emission computed tomography (SPECT) is a high sensitivity nuclear imaging technique using short half-life gamma emitting radioisotopes that can image the whole body. In comparison, optical fluorescence imaging can utilise agents that emit visible or near-IR photons and can be applied to both pre-clinical *in vivo* and cellular microscopy studies. However, it lacks the excellent tissue penetration offered by nuclear imaging modalities.

The combination of radioimaging and fluorescence imaging presents significant opportunities in the design of useful imaging agents.[3] Combined single molecule SPECT/fluorescence agents can provide early phase high sensitivity imaging of *in vivo* biodistribution using SPECT, followed by longitudinal optical imaging.[4] Additionally, PET or SPECT imaging can be used to identify diseased tissue non-invasively, which can then be accurately biopsied or surgically resected based upon the fluorescence imaging signal.[5–7]

The clinical use of ^{99m}Tc in SPECT imaging has been well established for many decades. ^{99m}Tc ($t_{1/2}$ = 6.01 h, γ = 142.7 keV) is a gamma emitting radioactive isotope which is used in >80% of clinical nuclear diagnostic imaging scans, with over 40 million SPECT scans carried out per year worldwide.[8] What is less well understood is the behaviour of Tc agents at the sub-cellular level, since the image resolution of SPECT does not allow such determinations. Therefore intrinsically luminescent or fluorescently tagged ^{99m}Tc SPECT agents[9] are potentially helpful in correlating *in vitro* and *in vivo* imaging properties,[10] and in determining their cellular uptake, trafficking and localisation.[11] From an inorganic chemistry perspective, non-radioactive rhenium is the obvious choice for developing structurally analogous and chemically related complexes.[12] Such an approach can be used to validate the development of appropriate chelates[13] for ^{99m}Tc and develop experimental protocols for synthesis and purification.[14] Indeed, rhenium complexes are now attracting considerable attention; in part for their potential as cancer therapy agents[15] as well as

[a]*School of Chemistry, Cardiff University, Main Building, Park Place, Cardiff CF10 3AT, Cymru/Wales, UK. E-mail: popesj@cardiff.ac.uk, s.j.archibald@hull.ac.uk*
[b]*Positron Emission Tomography Research Centre and Department of Biomedical Sciences, University of Hull, Cottingham Road, Hull, HU6 7RX UK*
[c]*Defence Science and Technology Laboratory, Porton Down, Salisbury, Wiltshire, UK*
†Electronic supplementary information (ESI) available. See DOI: 10.1039/c9dt04024b

the existence of accessible radioisotopes appropriate for radionuclide therapies/theranostic applications.[16] Binuclear Re(I) carbonyl complexes have shown accumulation in mitochondria leading to cell death.[17] Indeed a bimetallic Re(I)/^{99m}Tc(I) complex has also been described where the emissive nature of the Re(I) fragment can be exploited in optical studies.[18] In the case of fluorescently tagged rhenium complexes, these species can be assessed with respect to cellular uptake using conventional confocal fluorescence microscopy techniques.[19]

Whilst substituted 1,8-naphthalimides have been previously investigated in biological assays for their therapeutic applications,[20] more recent studies have shown that such species can also be very useful fluorophores for fluorescence bioimaging of cells.[21–23] The relative ease of functionalisation together with advantageous absorption and emission properties in the visible region have led to a large number of reports on their application to cell imaging. For example, recent studies have shown that the 1,8-naphthalimide structure can dictate intracellular localisation, including effective mitochondrial targeting.[24]

Since mitochondria have essential roles in energy production, cell signalling, cell-cycle control and cell death, and mitochondrial function can be disrupted in both ischaemic heart cells and cancer cells, they are attractive targets. Thus the development of a SPECT/fluorescence multimodal imaging agents for targeting mitochondria would therefore allow for *in vitro*, *in vivo* and *ex vivo* examination of myocardial function and tumour growth.[25] In this context, this current work describes the development of 1,8-naphthalimide functionalised chelates suitable for labelling with ^{99m}Tc(I) for mitochondrial targeted multimodal imaging. During the course of these studies, work by Turnbull *et al.* has shown that a series of related 4-amino-1,8-naphthalimide fluorophores can be complexed with Re(I)/^{99m}Tc(I). The overall charge of the complex was shown to strongly influence the biological attributes of the species.[26]

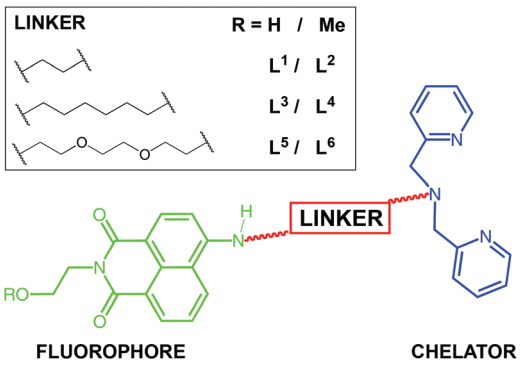

Scheme 1 Design aspects of the compounds synthesised in this study to provide a fluorophore functionalised chelate to the $\{M(CO)_3\}^+$ unit (M = ^{99m}Tc, Re). Six derivatives (L^{1-6}) were synthesised with three different linker units.

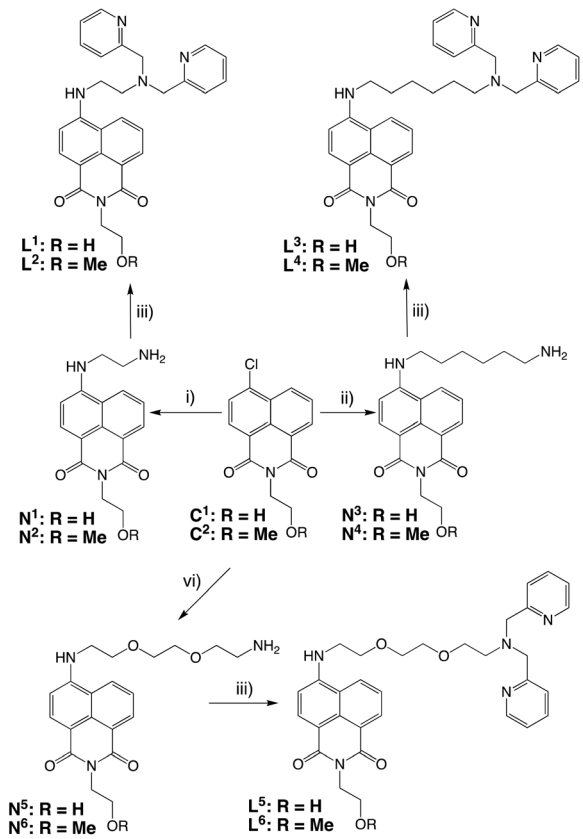

Scheme 2 Synthesis of the precursors and ligands. Reagents and conditions: (i) *N*-Boc-ethylenediamine, DMSO, heat; then TFA/DCM; (ii) 1,6-diaminohexane, DMSO, heat; (iii) 2-pyridinecarboxaldehyde, $NaBH(OAc)_3$, 1,2-dichloroethane; (iv) *N*-Boc(2,2′-(ethylenedioxy)diethylamine, DMSO, heat; then TFA/DCM.

Synthesis and characterisation of ligands and complexes

Scheme 1 shows the different chelator structures that were synthesised in this study. The compounds were designed to meet the coordination chemistry requirements of M(I) (where M = Re, Tc) with a face-capping tridentate donor set, fulfilled by a dipicolylamine (DPA)[27] chelating moiety. This is linked to the naphthalimide fluorophore for optical imaging *via* different length spacers of variable hydro- and lipophilicity. Thus, a series of six ligands were synthesised in three or four steps from 4-chloro-1,8-naphthalic anhydride (Scheme 2). Substitution at the 4-chloro position of the naphthalimide ring was achieved in DMSO at elevated temperature using an excess of diamine (often as the mono-Boc protected version). Following cleavage of the Boc group (trifluoroacetic acid in dichloromethane), treatment of $\mathbf{N^{1-6}}$ with 2-pyridinecarboxaldehyde in a one-pot reductive amination procedure gave the dipicolylamine derived target ligands, $\mathbf{L^{1-6}}$, in each case. All experimental details and spectroscopic characterisation data for the synthesis of intermediates and ligands are included in the Experimental section.

All isotopes of technetium are radioactive, and so natural rhenium is commonly used as a chemical analogue[28] to allow the synthetic and purification protocols to be optimised prior to the use of a radionuclide. The corresponding tricarbonyl Re(I) complexes were isolated by reacting[29] the precursor compounds with *fac*-$[Re(CO)_3(MeCN)_3]BF_4$ to yield *fac*-$[Re(CO)_3(L)]BF_4$ as air stable solids. Characterisation of the complexes was achieved using a range of spectroscopic and analytical techniques. The expected facial geometry with respect to the three carbonyl ligands was confirmed using IR spectroscopy. In all cases two C≡O stretches were observed between 2040–1900 cm^{-1} which are attributed to the pseudo C_{3v} symmetry of the complexes. In addition to this, the naphthalimide carbonyl stretches were observed at 1700–1625 cm^{-1} and the $[BF_4]^-$ counter anion at *ca.* 1055 cm^{-1}. High resolution mass spectrometry data were obtained for each complex identifying the cationic fragment with the appropriate isotopic distribution for rhenium. ^1H NMR spectroscopy was able to clearly establish the formation of the complex in each case. Firstly, the methylene linkers of the dipicolylamine unit shift upon coordination and become diastereotopic with an observed coupling around 16 Hz.[28] The aliphatic protons of the linker unit are also mildly shifted in the complex *versus* the ligand. The general pattern amongst the aromatic proton resonances is retained upon formation of the complex. Principally, data from ^{13}C NMR studies allowed identification, in all cases, of the rhenium-bound carbonyls (*ca.* 195 ppm) and the naphthalimide carbonyls (*ca.* 165 ppm).

Luminescence properties

Prior to radiolabelling and imaging studies, the electronic and optical properties of these species were investigated (Table 1). The UV-vis. spectra of all ligands were recorded in MeCN or chloroform solutions. Because of the relative hydrophilicity of the L^5/L^6 systems, additional data in aqueous solution was also obtained on these ligands and their complexes. The absorption spectra showed some common features, with higher energy absorptions associated with the naphthalimide and pyridyl based π–π* transitions, and a lower energy, broad peak around 440 nm which was assigned to an intramolecular charge transfer (ICT) transition from the amine-functionalised naphthalimide chromophore. The position of the ICT peak showed a slight shift that was dependent upon the amine substituent and was shown to be sensitive to the polarity of solvent, as expected for a charge transfer transition.[30] The absorption spectra of the corresponding Re(I) complexes (for example, Fig. 1) were comparable, with only minor shifts of the ICT band upon formation of the cationic Re(I) complex that are likely to be a result of the cationic charge perturbing the ICT transition.[31] Typically the molar absorption coefficients (Table 1) of the ICT bands in the complexes were in the range of 7000–20 000 M^{-1} cm^{-1}.

Steady state emission spectra were obtained using an irradiation wavelength of 425 nm, corresponding to direct excitation of the ICT band of the ligand. All ligands and complexes showed an intense, featureless luminescence peak at

Table 1 Solvent dependent intramolecular charge transfer absorption and emission data for the ligands and rhenium(I) complexes

Compound	λ_{abs} (ε/M^{-1} cm^{-1})/nm	λ_{em}/nm[a]	τ_{obs}/ns[b]	ϕ/%[c]
L^1	434 (9310)[d]	518[d]	11.1[d]	15[d]
	428 (7800)[e]	508[e]	9.8[e]	19[e]
L^2	436 (10 420)[d]	521[d]	10.5[d]	22[d]
	427 (8160)[e]	510[e]	8.5[e]	17[e]
L^3	433 (7300)[d]	518[d]	9.7[d]	28[d]
	435 (8240)[e]	508[e]	1.4, 8.8 (94%)[e]	28[e]
L^4	429 (8000)[d]	517[d]	9.5[d]	31[d]
	430 (18 600)[e]	505[e]	8.1[e]	35[e]
L^5	448 (10 220)[f]	542[f]	3.4, 6.0 (64%)[f]	39[f]
	429 (8910)[d]	521[d]	9.4[d]	12[d]
L^6	448 (2620)[f]	549[f]	5.4[f]	8[f]
	429 (7920)[d]	520[d]	9.7[d]	30[d]
$[Re(CO)_3(L^1)]BF_4$	430 (8560)[d]	515[d]	10.9[d]	67[d]
	432 (7510)[e]	503[e]	9.1[e]	23[e]
$[Re(CO)_3(L^2)]BF_4$	433 (19 200)[d]	519[d]	9.8[d]	30[d]
	430 (14 300)[e]	504[e]	9.2[e]	37[e]
$[Re(CO)_3(L^3)]BF_4$	430 (16 300)[d]	520[d]	9.8[d]	26[d]
	434 (10 100)[e]	512[e]	7.7[e]	29[e]
$[Re(CO)_3(L^4)]BF_4$	431 (13 020)[d]	517[d]	10.2[d]	40[d]
	425 (18 660)[e]	483[e]	8.0[e]	38[e]
$[Re(CO)_3(L^5)]BF_4$	446 (7190)[f]	540[f]	6.0[f]	49[f]
	429 (8100)[d]	526[d]	10.0[d]	15[d]
$[Re(CO)_3(L^6)]BF_4$	445 (10 700)[f]	539[f]	5.9[f]	57[f]
	448 (12 240)[d]	516[d]	11.1[d]	17[d]

[a] Measurements obtained in aerated solutions; λ_{ex} = 405 nm. [b] λ_{ex} = 295 nm. [c] Using aerated MeCN solution of $[Ru(bipy)_3](PF_6)_2$ as a reference. [d] In acetonitrile. [e] In chloroform. [f] In water.

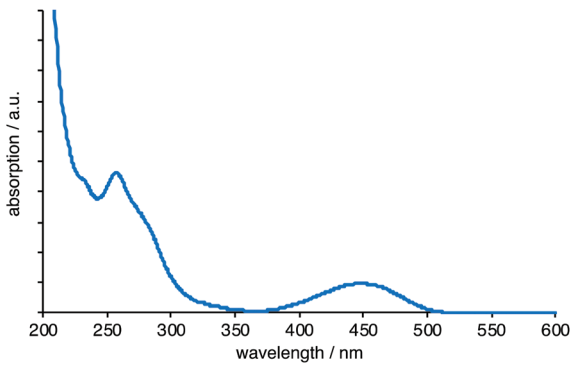

Fig. 1 UV-vis. absorption spectrum for *fac*-$[Re(CO)_3(L^5)]BF_4$ recorded in water.

505–550 nm, giving Stokes' shift >3500 cm^{-1}, which is typical of this class of fluorophore (for example, Fig. 2). Again, the position of the peak was found to be moderately sensitive to the amine substituent (related to the relative electron donating power) and the solvent polarity. For example, measurements in aqueous media for L^5/L^6 and their complexes resulted in a bathochromic shift of the emission maxima to *ca.* 540 nm, typical of positive solvatochromism (Fig. 2). Time-resolved experiments revealed lifetimes <15 ns in all cases, confirming the fluorescent nature of these ICT emitting species. Quantum yields were obtained for each species in the various solvents, and ranged 8–67%. For L^5/L^6 and their rhenium(I) complexes

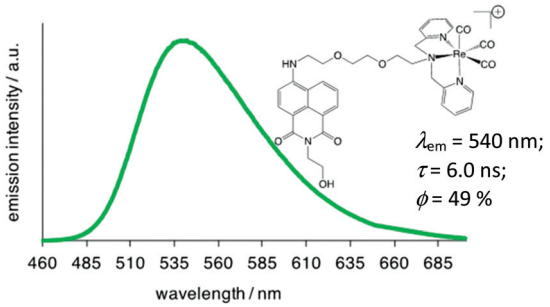

Fig. 2 Luminescence spectrum for *fac*-$[Re(CO)_3(L^5)]BF_4$ recorded in water (λ_{ex} = 425 nm).

these values were relatively high (around 50%) for the aqueous solutions. Taken together this gives a typical brightness value around 5000 M^{-1} cm^{-1}. The naphthalimide conjugated rhenium(I) complexes are thus well suited to cell imaging *via* confocal fluorescence microscopy, with visible fluorescence, good Stokes' shifts and relatively high quantum yields giving reasonably bright fluorophores.

Radiolabelling with technetium-99m

Having established the Re(I) coordination chemistry and the optical properties of the complexes, radiolabelling of selected ligand systems was attempted with the SPECT imaging (gamma emitting) isotope technetium-99m. Radiolabelling studies were conducted using *fac*-$[^{99m}Tc(CO)_3(H_2O)_3]^+$, which was obtained from the reduction of $[^{99m}TcO_4]^-$ using the method reported by Alberto *et al.*[32,33] Initial attempts to radiolabel $\mathbf{L^1}$ (the ligand variant with an ethylene linker between the naphthalimide and the dipicolylamine chelate unit) led to the formation of a number of radioactive species indicative, perhaps, of the decomposition of the ligand. Certainly, the limited aqueous solubility of $\mathbf{L^1}$ was likely to be a hindrance to efficient radiolabelling.

Therefore, the focus of further radiochemistry experiments was focussed upon the more hydrophilic naphthalimide $\mathbf{L^5}$ (the ligand variant incorporating the ethylenedioxodiamine linker) which demonstrated good water solubility.

Preliminary experiments with water-soluble $\mathbf{L^5}$ indicated much better radiolabelling yields and limited degradation (Fig. 3),[34] and therefore a range of conditions were tested to optimise the radiolabelling reaction (Table 2). Varying quantities of lyophilised $\mathbf{L^5}$ (15 to 300 μg), were radiolabelled with freshly reduced *fac*-$[^{99m}Tc(CO)_3(H_2O)_3]^+$ (10–40 MBq, 0.13–2.6 mM final precursor concentration, pH 7–8, buffered with 5 mM PBS) at 70 °C. The radiolabelling yield was determined by integration of radio-HPLC traces and, at 30 min, varied from 23% to 57%, plateauing at 55–57% for 30–150 μg (0.26–1.32 mM) range while declining to 43% when the amount of $\mathbf{L^5}$ was increased to 300 μg (2.0 mM). Increasing the reaction time to 60 min only had an effect on the lowest concentration (0.13 mM), with the yield increasing from 23% to 39%. Similarly, a three-fold increase of *fac*-$[^{99m}Tc(CO)_3(H_2O)_3]^+$ (up to 124–135 MBq) did not have any observable effect on the

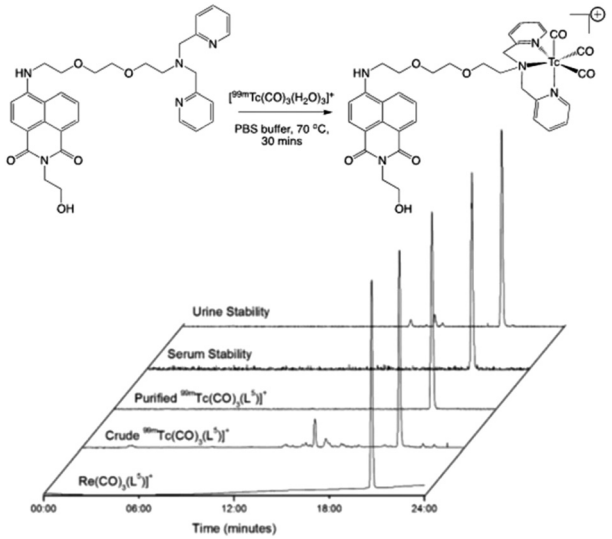

Fig. 3 Preparation (top) and stability assessments (bottom) of radiolabelled $\mathbf{L^5}$: comparative HPLC traces for *fac*-$[Re(CO)_3(L^5)]^+$ and *fac*-$[^{99m}Tc(CO)_3(L^5)]^+$.

Table 2 Radiochemical yields for the formation of *fac*-$[^{99m}Tc(CO)_3(L^5)]^+$

L^5 conc. (mM)	30 min	60 min	90 min
0.2	43	47	53
0.4	51	53	55
1.0	56	57	57
2.0	42	41	43

radiolabelling yield at 0.53–1.32 mM precursor concentrations. Thus, optimised $\mathbf{L^5}$ radiolabelling conditions were fixed at 0.53–1.32 mM precursor concentration, pH 7–8 (PBS), 70 °C, 30 min (Fig. 3).

Stability and mitochondrial uptake of *fac*-$[^{99m}Tc(CO)_3(L^5)]^+$

Lipophilicity is an important parameter in dictating the cellular localisation of organometallic complexes.[35] Lipophilicity ($\log D_{7.4}$) measurements were carried out on the radiolabelled species *fac*-$[^{99m}Tc(CO)_3(L^5)]^+$ and showed a value of 0.67 ± 0.06. This suggests a species with suitable solubility for biological studies, but passive cell membrane permeability is likely to be less favourable.[36] For drug-like species, such a value can also indicate that a renal clearance pathway will be observed.[37] To mimic *in vivo* conditions, formulated *fac*-$[^{99m}Tc(CO)_3(L^5)]^+$ was incubated with human serum at 37 °C. HPLC analysis did not reveal any significant instability up to 3 hours, indicating that the radiolabelled compound had sufficient stability to progress to preliminary *in vivo* imaging experiments.

To investigate *fac*-$[^{99m}Tc(CO)_3(L^5)]^+$ behaviour towards mitochondria, experiments were carried out using mitochondria freshly isolated from rat heart tissue. *fac*-$[^{99m}Tc(CO)_3(L^5)]^+$ accumulated in the mitochondria to a higher extent (55.68 ± 6.5%) than complexes containing the cationic triphenylpho-

sphonium mitochondria targeting group that has been frequently used in mitochondrial targeting.[38] This uptake was highly dependent on mitochondrial membrane potential (MMP) as shown by a nearly complete abrogation (1.35 ± 0.14%) when the MMP was depolarised using carbonyl cyanide *m*-chlorophenylhydrazine (CCCP).

Cell imaging studies with *fac*-[Re(CO)$_3$(L^5)]$^+$ and preliminary *in vivo* assessment of *fac*-[^{99m}Tc(CO)$_3$(L^5)]$^+$

Cellular cytotoxicity was assessed using U87 cells *in vitro* by the MTT assay, giving a CC_{50} value of 72.7 μM (Fig. 4), which indicates low cytotoxicity *in vitro* for the compound. Whole cell mitochondrial uptake of *fac*-[Re(CO)$_3$(L^5)]$^+$ was then studied using confocal fluorescence microscopy in human breast cancer cells (MCF-7) in culture. As a control, a benzyl chloride based mitochondrial stain (MitoTracker deep red, MDR) was used for dye co-localisation studies as its emission wavelength (665 nm) is sufficiently different from *fac*-[Re(CO)$_3$(L^5)]$^+$ (540 nm) thus allowing independent detection. Confocal fluorescence microscopy studies into the mitochondrial localisation for *fac*-[Re(CO)$_3$(L^5)]$^+$ with MCF-7 cells gave an overlap coefficient of 0.66 (Fig. 5) suggesting a good degree of co-localisation.

Having established the mitochondrial and cellular uptake properties, a scoping *in vivo* experiment was carried out with *fac*-[^{99m}Tc(CO)$_3$(L^5)]$^+$ in a naïve mouse using SPECT/CT imaging (Fig. 6). Firstly, there were no signs of toxicity to the mouse during the *in vivo* studies. The tracer showed rapid clearance, predominantly *via* the biliary system along with a moderate amount cleared renally. This is consistent with the log *D* of *fac*-[^{99m}Tc(CO)$_3$(L^5)]$^+$, as some renal clearance was observed and more complex active transport mechanisms can influence hepatobiliary clearance.[39] Urine analysis demonstrated that the tracer was of a relatively high stability (85.4 ± 1.4%) and suitable for further *in vivo* analysis. From these imaging studies, it was clear that cardiac uptake was not observed for *fac*-[^{99m}Tc(CO)$_3$(L^5)]$^+$. This suggests that in its current form the tracer will not be appropriate for assessing cardiac function *in vivo* and so structural modification would be required to ensure uptake and retention.

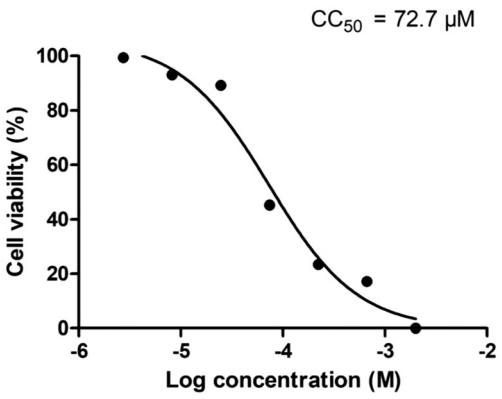

Fig. 4 Cell viability assay (MTT) result for *fac*-[Re(CO)$_3$(L^5)]$^+$.

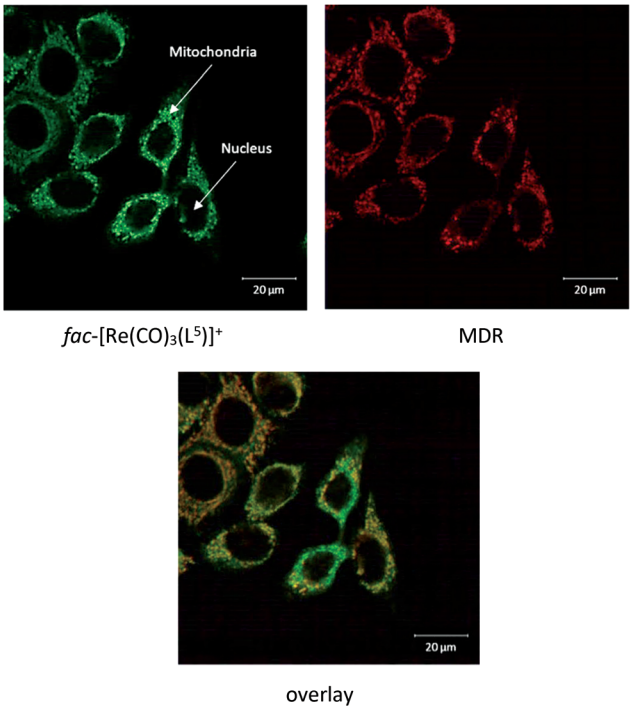

Fig. 5 Confocal fluorescence microscopy images of MCF-7 cells incubated with *fac*-[Re(CO)$_3$(L^5)]$^+$ (top left) and MitoTracker deep red (top right) and overlay (bottom; overlap coefficient = 0.66).

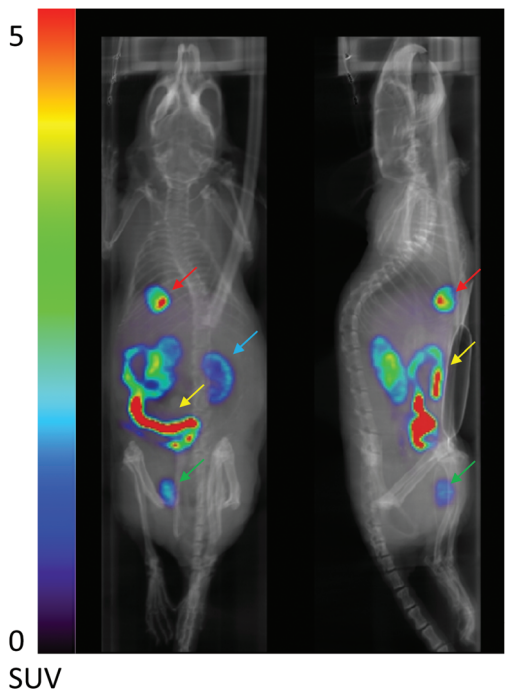

Fig. 6 SPECT and CT overlaid images with the SPECT images acquired using the radiotracer *fac*-[^{99m}Tc(CO)$_3$(L^5)]$^+$. Sagittal and coronal views show the localisation of the tracer after 22–60 min. Red arrow: gall bladder; yellow arrow: biliary clearance into the biliary tract and small intestine; green arrow: bladder; blue arrow: kidney.

Conclusions

In conclusion, this study shows the design, synthesis and characterisation of a new class of radiotracer which is preferentially taken up into the mitochondria of cells. The tracer combines a naphthalimide fluorophore with a technetium(I) tricarbonyl unit to give a structure with excellent cellular and mitochondrial uptake characteristics. Cellular bioimaging shows good image quality in the MCF-7 cell line. The preliminary *in vivo* assessment of the aqueous soluble ^{99m}Tc(I) compound shows rapid clearance, aligning with the requirements for nuclear imaging to ensure background signal is minimised. These results now justify further investigation of the tumour uptake properties *in vivo* with appropriate tumour models and larger animal cohorts.

In its current form, *fac*-[^{99m}Tc(CO)$_3$(**L**^{5})]$^+$ does not demonstrate cardiac uptake *in vivo*. Therefore, our further studies will also consider structurally modified variants that can promote and optimise this characteristic. During the course of these studies, Luyt and co-workers reported a peptide-functionalised naphthalimide-based fluorophore that can be used to target CXCR4 expressing cells for potential dual mode imaging.[40] This further suggests that the inherent fluorophore–chelate design presented herein holds great promise for future biological and bioimaging applications.

Experimental

General considerations

All reagents and solvents were commercially available and were used without further purification if not stated otherwise. For the measurement of ^{1}H and ^{13}C NMR spectra a Bruker Fourier^{300} (300 MHz), Bruker AVANCE HD III equipped with a BFFO SmartProbe™ (400 MHz) or Bruker AVANCE III HD with BBO Prodigy CryoProbe (500 MHz) was used. The obtained chemical shifts δ are reported in ppm and are referenced to the residual solvent signal. Spin–spin coupling constants J are given in Hz.

Low-resolution mass spectra were obtained by the staff at Cardiff University. High-resolution mass spectra were carried out at the EPSRC National Mass Spectrometry Facility at Swansea University. High resolution mass spectral (HRMS) data were obtained on a Waters MALDI-TOF mx at Cardiff University or on a Thermo Scientific LTQ Orbitrap XL by the EPSRC UK National Mass Spectrometry Facility at Swansea University. IR spectra were obtained from a Shimadzu IR-Affinity-1S FTIR. Reference to spectroscopic data are given for known compounds. UV-Vis studies were performed on a Shimadzu UV-1800 spectrophotometer as MeCN solutions (2.5 or 5 × 10^{-5} M). Photophysical data were obtained on a JobinYvon–Horiba Fluorolog spectrometer fitted with a JY TBX picosecond photodetection module as MeCN solutions. Quantum yield measurements were obtained on aerated MeCN solutions of the complexes using [Ru(bpy)$_3$](PF$_6$)$_2$ in aerated MeCN as a standard (Φ = 0.016). Emission spectra were uncorrected and excitation spectra were instrument corrected. The pulsed source was a nano-LED configured for 295 nm or 372 nm output operating at 1 MHz. Luminescence lifetime profiles were obtained using the JobinYvon–Horiba FluoroHub single photon counting module and the data fits yielded the lifetime values using the provided DAS6 deconvolution software.

Standard radiolabelling protocol

All work carried out with ionising radiations was carried out within the legal requirements of the Ionising Radiations Regulations 2017 and the Environmental Permitting Regulations 2010. The studies followed local rules and regulations to ensure safe and compliant handling of open source radioactive materials. The labelling precursor in a glass HPLC vial was dissolved in 50 μL of MeOH and was further diluted with 100 μL of 10 mM PBS solution. The solution was degassed by sonication and purged with argon for 10 min. Up to ~400 MBq of freshly reduced *fac*-[^{99m}Tc(CO)$_3$(H$_2$O)$_3$]$^+$ in a reduction medium (~500 μL) was added, bringing the final precursor concentration to previously determined optimum 0.5–1.3 mM concentration range. The reaction mixture was incubated in a heating shaker at 70 °C mixing at 600 rpm for 30 min. After which it was cooled down to room temperature and injected onto semi-preparatory HPLC (ACE5 C18 5 Å 100 × 250). Product containing fraction (RCY = 47 ± 18%, n = 3, corrected for decay to the beginning of reaction) eluting at 12–14 min was collected, diluted twice with deionised water and loaded onto homemade SPE cartridge (Sep-Pak Light) containing 80–100 mg of Oasis C18 sorbent. The cartridge was washed with 2–3 mL of deionised water and dried by a current of inert gas. The product was eluted by 500 μL of ethanol, the solvent was evaporated under gentle heating aided by a current of inert gas and reformulated into PBS. For *in vivo* evaluation, the formulation was filtered using a 0.22 μm filter for sterility prior to animal administration. The decay corrected preparatory yield was 21 ± 11% (n = 3) and the full process requires less than 2 h from the start of synthesis.

Lipophilicity

Log P was measured using a standard shake-flask method. Briefly, an aliquot of the tracer solution in ethanol (~1 MBq) was dried in a 1.5 mL Eppendorf tube and dissolved in 1 mL of 1 : 1 mixture of octanol/PBS. Solution was vigorously mixed in vortex shaker for 5 min at room temperature and phases separated by centrifugation at 14.5 krpm for 2 min. 50 μL of each phase was diluted up to 1 mL and measured using an AGC.

Serum stability

An aliquot of the tracer in ethanol (~3 MBq) was dried, dissolved in 0.5 mL of human blood serum in a HPLC vial and incubated while shaking at 600 rpm at 37 °C up to 3 hours. Samples were taken at time 0, 30 min, 60 min, 1 h, 2 h and 3 h; the protein was precipitated by addition of double volume of ice cold methanol and removed by centrifugation and the supernatant analysed by radio-HPLC.

In vivo SPECT imaging and stability

All animal procedures were approved by the University of Hull Animal Welfare Ethical Review Body (AWERB) and carried out in accordance with the Animals in Scientific Procedures Act 1986 and the UKCCCR Guideline 2010[41] by approved protocols following institutional guidelines (Home Office Project License number 60/4549 held by Dr Cawthorne).

Female CD1 nude mice (25–30 g, Charles River, UK) were induced with 5% and maintained under anaesthesia with 3% isoflurane (oxygen at 1 L min^{-1}). Temperature and respiration were monitored throughout the scan. SPECT-CT acquisition was carried out on a Mediso NanoSPECT/CTPLUS, equipped with multi-pinhole pyramid collimators. Animals were injected i.v. with ≈30 MBq (200 μL) of *fac*-$[^{99m}Tc(CO)_3(\mathbf{L}^5)]^+$ 30 min prior to a 25 min SPECT scan (energy window: 126.4–154.6 keV). To show anatomical co-registration, a CT scan (240 projections, 1 s exposure, 55 kVp X-rays) was acquired following the SPECT scan. SPECT and CT images were reconstructed with an iterative algorithm and with exact cone beam Filtered Back Projection, respectively (HiSPECT, Scivis GmbH, Germany).

After imaging experiments, mice urine was collected, proteins were precipitated by addition of double volume of ice cold methanol and removed by centrifugation at 14.5 krpm for 5 min and supernatant was analysed by radio-HPLC indicating 85.4 ± 1.4% stability (n = 1, triplicate analyses).

In vitro analysis

Cell culture. MCF-7 cells were purchased from the European Collection of Cell Cultures and grown in RPMI-1640 media. Media was supplemented with 10% fetal calf serum (FCS). Human glioblastoma cell line from (U87) from ATCC and it was cultured using DMDM media with 10% (v/v) heat inactivated fetal bovine serum (FBS). Media and FCS were purchased from Gibco/Life Technologies, UK. Cells were maintained in Nunc 75 cm^2 tissue culture flasks (Fischer Scientific, UK) inside a humidified 5% CO_2 incubator at 37 °C. Both cell lines were divided bi-weekly for maintenance of stock at a divided ratio of 1 : 8–1 : 10 for MCF-7 cells. For confocal and flow cytometry experiments cells were counted and seeding densities (below) were used.

Toxicity. Cells were seeded in 96 well plate with 1000 cells per well in 200 μl growth medium. The plates were incubated overnight at 37 °C allow cells to adhere. After 18 h media was removed from the wells and 100 μl of treated media with various concentrations of compounds was added. The plates were returned to the incubator. After 72 h, MTS reagent (Promega, UK) 20 μl was added to the wells. Plates were incubated for 3 h at 37 °C. Absorbance reading were taken at 490 nm using Synergy HT microplate reader (Biotek, USA). The absorbance value of each triplicate were averaged and the media only absorbance was subtracted. Compounds reading were normalised to the control reading. Empty plate and compound added background analysis was carried out to ensure low levels of non-specific fluorescence.

Flow cytometry. 1×10^5 cells per well were seeded in six-well plates and cultured for 2–3 days until 70–80% confluent. Cell media was removed and 1 mL 0.1% FCS-containing media was added. Carbonyl cyanide *m*-chlorophenylhydrazone (CCCP, Sigma Aldrich, UK) in DMSO (50 mM, 1 μL) was added into three wells (1 mL total volume) and 0.1% DMSO was added to the remaining three control wells (as a control). Plates were placed inside a CO_2 incubator for 30 min, followed by the addition of compound (500 nM, 50 μL media) to both groups. Plates were incubated inside the CO_2 incubator at 37 °C for 1 hour, subsequently, media was removed and the cells were washed twice with ice cold PBS buffer. Cells were harvested into PBS with cell scrapper and isolated by centrifugation at 200*g* for 5 min at 4 °C. The pellet was re-suspended in 300 μL of PBS and the cell suspension transferred into polypropylene FACS tubes (Falcon 2054) and analysed by a FACScan flow cytometer (BD Biosciences Europe, Erembodegem, Belgium). Dot plot was used to gate cells and the FL-1 channel was used to measure variation in fluorescence intensities. Mean fluorescence intensities were used to quantify for comparison.

Confocal microscopy. MCF-7 cells (2.5×10^3) and H9c2 cells (4×10^3) were seeded in Mattak confocal dishes (P35G-1.2-20-C, 35 mm^2) and cultured for 2–3 days until 70–80% confluent. After reaching desired cell density, the growth media was replaced with 1 mL 0.1% FCS-containing media and cells were treated with *fac*-$[Re(CO)_3(\mathbf{L}^5)]^+$ (500 nM, 50 μL) for 1 hour inside a CO_2 incubator under 5% CO_2. Mitotracker deep red (MDR, 250 nM, 20 μL) was added 1 hour prior to compound to obtain double labelled cells for mitochondrial co-localisation study. After 30 min, the cells were washed twice with 1 mL PBS and media containing 15 mM HEPES was added. Unstained control samples of cells were used to check for auto fluorescence. Live cell images were obtained using ZEN software on a Zeiss LSM 710 inverted confocal microscope, equipped with an incubator chamber at 37 °C. Images were obtained using a Zeiss 63× water objective.

To measure the degree of overlap between subcellular localisation of *fac*-$[Re(CO)_3(\mathbf{L}^5)]^+$ and MDR, a colocalisation coefficient was calculated following standard methods. Single-label control samples were prepared to eliminate fluorescence overlap between two fluorescence channels; in addition to *fac*-$[Re(CO)_3(\mathbf{L}^5)]^+$ or MDR, untreated cells were assessed in order to eliminate background fluorescence. Single-label control samples were imaged under the same exposure settings as double-labelled samples. Exact coordinates were determined using crosshairs at X and Y coordinates from single-labelled controls and were identical for double-labelled samples. Once the exact coordinates were determined, the ZEN software gave tables containing values of co-localisation coefficient and overlap coefficient.

Mitochondrial uptake of $[^{99m}Tc(CO)_3(\mathbf{L}^5)]^+$. Cardiac mitochondria were isolated following a modified method based on that reported by Boehm *et al.*[42] A male Sprague–Dawley rat was anaesthetised with Dolethal and the heart was excised, washed and trimmed in cold buffer. The trimmed heart was transferred into a centrifuge tube containing 5 ml of ice cold buffer and then minced. The minced cardiac tissue suspension was

transferred to a Teflon glass homogeniser (Scientific Laboratory Supplies, UK) and a further 5 ml of ice cold buffer A was added (total 10 ml). 1 ml trypsin was added and gently homogenized using a tight fitting Teflon pestle (Scientific Laboratory Supplies, UK). After 15 min of trypsin digestion, 10 ml of trypsin inhibitor was added and mixed with three passes of the tight fitting Teflon pestle. The tissue suspension was then centrifuged at 600*g* for 10 min at 4 °C. The supernatant was transferred into another centrifuge tube and centrifuged again at 8000*g* for 10 min at 4 °C. The resultant pellet was resuspended in 10 ml of isolation buffer B and again centrifuged at 8000*g* for 10 min at 4 °C. The mitochondrial pellet was then resuspended in 100 μl of respiratory buffer containing 10 mM succinate. The total protein content of the isolated mitochondria was measured using Bio-Rad protein assay. 10 μl of the isolated mitochondria suspension was added into 390 μl of water (40 times dilution). A standard solution was made with BSA to calibrate the protein amount. 60 μl of the mitochondria suspension was added to 3 ml of Bio-Rad solution and 60 μl from each of the BSA stock solution dilutions were also taken and added to 3 ml of Bio-Rad solution.

Mitochondrial protein concentration was shown to be 1.23 μg μl^{-1}, as it was 40 times diluted, the original concentration was 49.46 μg μl^{-1}. Hence, the total mitochondrial protein amount was 4946 μg in 100 μl. 150 μg protein was aliquoted into each Eppendorf. 100 μl of respiratory buffer containing 10 mM succinate added to give the control (n = 3 for each tracer). 10 μM CCCP was added into 100 μl of respiratory buffer containing 10 mM succinate and was then added in remaining Eppendorf tubes. All the Eppendorf tubes were transferred into the CO_2 incubator containing 5% CO_2 at 37 °C for 15 min and after that 0.5 MBq of tracer was added to the control and CCCP treated mitochondria. All of the Eppendorf tubes were transferred back into the CO_2 incubator for 30 min and after that the assay was terminated by centrifugation at 8000*g* for 5 min at 4 °C. The supernatant was collected and the mitochondrial pellet was washed three times with ice cold respiratory buffer containing 10 mM succinate. After the final wash, the mitochondrial pellet was resuspended into 1 ml of PBS. The amount of radioactivity was measured using the gamma counter (PerkinElmer Wallac wizard 3″). Percent accumulation was quantified by using the ratio of activity in pellet to that in the pellet plus supernatant. The experiment was carried out three times using internal triplicates. The data is presented as an average of each internal triplicate with the standard deviation among triplicates.

Ligands and precursors

Synthesis of compound C^1.[43] 4-Chloro-1,8-naphthalic anhydride (2 g, 8.6 mmol) was dissolved in ethanol (60 mL) and ethanolamine (0.79 mL, 12.9 mmol) was added. The solution was then heated at reflux for 12 h under a nitrogen atmosphere. Upon cooling to 0 °C precipitation occurred, and filtration yielded **C^1** as a yellow solid (2.01 g, 85%). ^{1}H NMR (400 MHz, $CDCl_3$): δ_H 8.70 (d, J = 6.8 Hz, 1H), 8.64 (d, J = 8.4 Hz, 1H), 8.54 (d, J = 7.6 Hz, 1H), 7.88 (m, 2H), 4.48 (t, J = 4.8 Hz, 2H), 4.01 (t, J = 4.8 Hz, 2H) ppm. LRMS ES^+ found m/z = 275.03 $[M^+]$.

Synthesis of compound C^2.[44] Prepared as for **C^1** except using 2-methoxyethylamine (0.90 g, 12.9 mmol), yielding **C^2** as a yellow solid (1.96 g, 79%). ^{1}H NMR (400 MHz, $CDCl_3$): δ_H 8.68 (d, J = 7.0 Hz, 1H), 8.61 (d, J = 8.1 Hz, 1H), 8.52 (d, J = 8.2 Hz, 1H), 7.91–7.80 (m, 2H), 4.44 (t, J = 5.7 Hz, 2H), 3.73 (t, J = 5.7 Hz, 2H), 3.38 (s, 3H) ppm. LRMS ES^+ found m/z = 289.05 $[M^+]$.

Synthesis of N^1. **C^1** (0.3 g, 1.01 mmol) was dissolved in DMSO (4 mL) and *N*-Boc-ethylenediamine was added (0.47 g, 2.93 mmol) and the solution heated at reflux for 16 hours under a nitrogen atmosphere. The solution was flooded with 30 mL of water and neutralised with 0.1 M HCl. The product was then extracted with dichloromethane (3 × 15 mL) and washed with water (3 × 10 mL) and brine (3 × 10 mL). The solvent was then reduced to a minimum and precipitation induced by the dropwise addition of petroleum ether. Filtration of the precipitate followed by washing with diethyl ether (5 mL) yielded the Boc-protected intermediate product as a bright orange solid (0.27 g, 65%). ^{1}H NMR (300 MHz, $CDCl_3$): δ_H 8.55 (d, J = 7.3 Hz, 1H), 8.42 (d, J = 8.5 Hz, 1H), 8.27 (d, J = 8.3 Hz, 1H), 7.59 (t, J = 7.7 Hz, 1H), 7.19 (s, 1H), 6.55 (d, J = 8.3 Hz, 1H), 4.45 (t, J = 4.3 Hz, 2H), 3.97 (s, 2H), 3.65 (dd, J = 10.2, 5.3 Hz, 2H), 3.49–3.38 (m, 2H), 1.42 (s, 9H) ppm. ^{13}C $\{^1$H$\}$ NMR (101 MHz, $CDCl_3$): δ_C 163.89, 163.10, 150.08, 134.03, 130.78, 129.32, 128.73, 124.48, 121.99, 120.37, 108.76, 103.95, 57.96, 41.47, 40.36, 37.31 ppm. LRMS ES^+ found m/z = 400.19 $[M + H]^+$. Deprotection of the intermediate product was achieved by stirring the solution of the intermediate in 50% TFA in DCM for 24 hours under a nitrogen atmosphere. The solvents were then removed under vacuum, and the residue dissolved in methanol and the solvent removed again. This was repeated in triplicate to yield the final product as an oily yellow solid (0.178 g, 60%). ^{1}H NMR (300 MHz, d_6-DMSO): δ_H 8.63 (d, J = 8.3 Hz, 2H), 8.42 (d, J = 7.2 Hz, 2H), 8.26 (d, J = 8.4 Hz, 2H), 7.78 (s, 2H), 7.69 (t, J = 7.8 Hz, 2H), 6.84 (d, J = 8.5 Hz, 2H), 4.84 (s, J = 46.7 Hz, 2H), 4.11 (t, J = 6.3 Hz, 4H), 3.73–3.51 (m, 8H), 3.39 (s, 2H), 3.17 (s, 4H) ppm. ^{13}C$\{^1$H$\}$ NMR (101 MHz, d_6-DMSO): δ_C 163.89, 163.10, 150.08, 134.03, 130.78, 129.32, 128.73, 124.48, 121.99, 120.37, 108.76, 103.95, 57.96, 41.47, 40.36, 37.31 ppm. LRMS ES^+ found m/z = 332.12 $[M + Na]^+$. HRMS expected m/z = 322.1162 for $[M + Na]^+$ found m/z = 322.1163.

Synthesis of N^2. Prepared as for **N^1** but using **C^2** (0.3 g, 1.0 mmol), yielding the intermediate product as a bright orange solid (0.157 g, 38%). ^{1}H NMR (400 MHz, $CDCl_3$): δ_H 8.51 (d, J = 7.3 Hz, 1H), 8.38 (d, J = 8.4 Hz, 1H), 8.20 (d, J = 8.4 Hz, 1H), 7.54 (t, J = 7.5 Hz, 1H), 7.02 (s, 1H), 6.50 (d, J = 8.3 Hz, 1H), 5.03 (s, 1H), 4.36 (t, J = 5.6 Hz, 2H), 3.65 (t, J = 5.7 Hz, 2H), 3.58 (s, 2H), 3.39 (s, 2H), 3.32 (s, 3H), 1.41 (s, 8H) ppm. ^{13}C$\{^1$H$\}$ NMR (101 MHz, $CDCl_3$): δ_C 164.33, 158.65, 150.24, 134.77, 131.32, 129.94, 127.14, 124.71, 122.77, 120.39, 103.30, 80.85, 77.24, 69.84, 58.80, 46.87, 39.50, 38.96, 28.37 ppm. LRMS found m/z = 414.20 $[M + H]^+$. Deprotection yielded the final product as an orange oil (0.103 g, 87%). ^{1}H NMR

(400 MHz, CD_3OD): δ_H 8.41 (d, J = 7.6 Hz, 2H), 8.28 (d, J = 8.8 Hz, 1H), 7.65–7.49 (m, 2H), 6.78 (d, J = 8.7 Hz, 1H), 4.24 (t, J = 6.0 Hz, 2H), 3.69 (t, J = 6.1 Hz, 2H), 3.59 (t, J = 6.0 Hz, 2H), 3.27 (m, 2H), 3.25 (s, 3H) ppm. LRMS found m/z = 336.13 $[M + Na]^+$. HRMS expected m/z = 336.1319 for $[M + Na]^+$, found m/z = 336.1320.

Synthesis of N³. **C¹** (0.75 g, 2.73 mmol) was dissolved in DMSO (4 mL) and 1,6 diaminohexane (0.4 mL, 4.1 mmol) was added and the solution heated at reflux for 16 hours. The solution was flooded with 30 mL of water and neutralised with 0.1 M HCl. The product was then extracted with dichloromethane (3 × 15 mL) and washed with water (3 × 10 mL) and brine (3 × 10 mL). The solvent was then reduced to a minimum and precipitation induced by the dropwise addition of petroleum ether. Filtration of the precipitate followed by washing with diethyl ether (5 mL) yielded the product as an orange solid (0.422 g, 44%). ^{1}H NMR (300 MHz, $CDCl_3$): δ_H 8.58 (d, J = 7.4 Hz, 1H), 8.46 (d, J = 7.6 Hz, 1H), 8.10 (d, J = 8.1 Hz, 1H), 7.69–7.57 (m, 1H), 6.75–6.66 (m, 1H), 5.36 (s, 1H), 4.51–4.40 (m, 2H), 4.03–3.92 (m, 2H), 3.50–3.34 (m, 2H), 2.78–2.67 (m, 2H), 1.95–1.75 (m, 2H), 1.65–1.41 (m, 6H) ppm. $^{13}C\{^1H\}$ NMR (126 MHz, $CDCl_3$): δ_C 165.58, 165.01, 150.88, 135.09, 131.38, 130.03, 127.61, 124.36, 122.09, 120.31, 108.23, 104.03, 60.41, 43.27, 42.02, 41.22, 32.52, 28.28, 26.80, 26.41. LRMS found m/z = 356.20 $[M + H]^+$, HRMS expected m/z = 356.1896 found m/z = 356.1965.

Synthesis of N⁴. Prepared as for **N³** but using **C²** (0.75 g, 1.38 mmol) yielding the product as an orange solid (0.420 g, 42%). ^{1}H NMR (400 MHz, $CDCl_3$): δ_H 8.59 (d, J = 7.4 Hz, 1H), 8.47 (d, J = 8.3 Hz, 1H), 8.09 (d, J = 8.4 Hz, 1H), 7.63 (d, J = 7.7 Hz, 1H), 6.72 (d, J = 8.2 Hz, 1H), 5.32 (s, 1H), 4.45 (t, J = 5.8 Hz, 2H), 3.75 (t, J = 5.8 Hz, 2H), 3.57–3.30 (m, 5H), 2.74 (t, J = 6.6 Hz, 2H), 1.91–1.75 (m, 2H), 1.61–1.39 (m, 6H) ppm. $^{13}C\{^1H\}$ NMR (126 MHz, $CDCl_3$): δ_C 165.04, 164.97, 164.41, 150.14, 149.91, 134.82, 134.74, 131.30, 129.94, 129.87, 126.81, 126.50, 124.56, 124.49, 122.62, 122.55, 120.21, 120.16, 109.40, 109.14, 104.15, 104.09, 69.71, 58.66, 43.33, 41.19, 38.87, 28.62, 28.47, 26.90, 26.81, 26.40. LRMS found m/z = 370.21 $[M + H]^+$. HRMS expected m/z = 370.2127 for $[M + H]^+$, found m/z = 370.2125.

Synthesis of N⁵. **C¹** (0.75 g, 2.72 mmol) was dissolved in DMSO (5 mL) and *N*-Boc(2,2′-(ethylenedioxy)diethylamine (1.4 g, 5.64 mmol) was added and the solution heated at reflux for 16 hours under a nitrogen atmosphere. Upon being allowed to cool the solution was flooded with 30 mL of water and neutralised with 0.1 M HCl. The product was then extracted with dichloromethane (3 × 15 mL) and washed with water (3 × 10 mL) and brine (3 × 10 mL). The crude intermediate product was then purified further though the use of silica gel column chromatography using 3 : 2 acetone hexane with 4% triethylamine as the eluent. The solvents were then removed under vacuum yielding the intermediate product as a red oil (0.40 g, 30%). ^{1}H NMR (300 MHz, $CDCl_3$): δ_H 8.37 (d, J = 6.8 Hz, 1H), 8.28 (d, J = 8.4 Hz, 1H), 8.08 (d, J = 8.1 Hz, 1H), 7.46 (t, J = 7.5 Hz, 1H), 6.53 (d, J = 8.4 Hz, 1H), 6.03 (s, 1H), 5.00 (s, 1H), 4.36 (t, J = 4.8 Hz, 2H), 3.92 (t, J = 4.5 Hz, 2H), 3.82 (t, J = 5.1 Hz 2H), 3.64 (m, 4H), 3.57–3.45 (m, 4H), 3.28 (d, J = 4.8 Hz, 2H), 1.34 (s, 9H) ppm. LRMS found m/z = 389.18 $[M + H]^+$. Deprotection of the intermediate product was achieved by stirring in 50% TFA in DCM (10 mL) for 24 hours under a nitrogen atmosphere. The solvents were then removed under vacuum, and the residue dissolved in methanol and the solvent removed again. This was repeated in triplicate to yield **N⁵** as a red oil (0.29 g, 91%). ^{1}H NMR (300 MHz, CD_3OD): δ_H 8.31–8.19 (m, 2H), 8.09 (m, 1H), 7.43 (m, 1H), 6.61 (m, 1H), 4.23 (m, 2H), 3.80 (t, J = 5.1 Hz, 2H), 3.72–3.64 (m, 6H), 3.59–3.51 (m, 2H), 3.30–3.25 (m, 2H), 3.11–3.01 (m, 2H) ppm. $^{13}C\{^1H\}$ NMR (75 MHz, CD_3OD): δ_C 164.78, 150.78, 149.04, 134.14, 133.04, 130.55, 128.31, 128.01, 127.62, 123.86, 108.00, 103.65, 70.03, 68.62, 66.54, 59.03, 42.69, 39.22 ppm. LRMS found m/z = 388.18 $[M + H]^+$. HRMS expected m/z = 388.1872 for $[M + H]^+$, found m/z = 388.1857.

Synthesis of N⁶. Prepared as for **N⁵** but using **C²** (0.75 g, 2.59 mmol), first yielding the intermediate product as a red oil (0.46 g, 35%). ^{1}H NMR (400 MHz, MeOD) δ 8.35 (d, J = 7.8 Hz, 1H), 8.19 (d, J = 8.6 Hz, 1H), 7.50 (t, J = 7.9 Hz, 1H), 6.70 (d, J = 8.6 Hz, 1H), 4.23 (t, J = 6.1 Hz, 1H), 3.75 (t, J = 5.5 Hz, 1H), 3.67–3.62 (m, 1H), 3.62–3.55 (m, 8H), 3.27 (s, 1H), 2.96 (t, J = 5.1 Hz, 1H), 1.36 (s, 9H) ppm. Deprotection yielded the **N⁵** as a red oil (0.32 g, 88%). ^{1}H NMR (400 MHz, CD_3OD): δ_H 8.35 (d, J = 7.8 Hz, 2H), 8.19 (d, J = 8.6 Hz, 1H), 7.50 (app. t, J = 7.9 Hz, 1H), 6.70 (d, J = 8.6 Hz, 1H), 4.23 (t, J = 6.1 Hz, 2H), 3.75 (t, J = 5.5 Hz, 2H), 3.67–3.62 (m, 2H), 3.62–3.55 (m, 8H), 3.27 (s, 3H), 2.96 (m, J = 5.1 Hz, 2H) ppm. $^{13}C\{^1H\}$ NMR (400 MHz, CD_3OD): δ_C 116.2, 165.6, 152.4, 135.7, 132.2, 131.0, 139.2, 125.5, 123.2, 121.7, 109.5, 105.2, 71.6, 71.4, 70.7, 70.1, 67.9, 58.9, 44.2, 40.5, 39.7 ppm. LRMS found m/z = 402.20 $[M + H]^+$. HRMS expected m/z = 402.2023 for $[M + H]^+$, found m/z = 402.2017.

Synthesis of L¹. N¹ (0.11 g, 0.37 mmol) was dissolved in 1,2-dichloroethane and 2-pyridinecarboxaldehyde (0.07 mL, 0.74 mmol) was added and the solution stirred for 2 hours under a nitrogen atmosphere. Sodium trisacetoxyborohydride (0.24 g, 1.11 mmol) was then added and the solution stirred at room temperature for 18 hours. The solution was then neutralised with saturated $NaHCO_3$ and the product extracted into chloroform, washed with water (3 × 20 mL) and brine (3 × 20 mL). The organic layer was collected then dried over $MgSO_4$ and filtered, and the solvent removed to yield the product as an orange oil (0.13 g, 73%). ^{1}H NMR (400 MHz, $CDCl_3$): δ_H 8.80 (d, J = 8.9 Hz, 1H), 8.57 (d, J = 7.3 Hz, 1H), 8.52–8.49 (m, 2H), 8.35 (d, J = 8.6 Hz, 1H), 7.98 (s, 1H), 7.68–7.60 (m, 1H), 7.55–7.47 (m, 2H), 7.31 (d, J = 7.6 Hz, 2H), 7.12–7.07 (m, 2H), 6.48 (d, J = 8.1 Hz, 1H), 4.70 (s, 1H), 4.43–4.38 (m, 2H), 3.95 (s, 4H), 3.93–3.89 (m, 2H), 3.36–3.31 (m, 2H), 3.01–2.96 (m, 2H) ppm. $^{13}C\{^1H\}$ NMR (151 MHz, $CDCl_3$): δ_C 164.76, 164.11, 160.85, 150.53, 140.25, 134.54, 131.29, 129.82, 127.09, 125.21, 125.00, 124.53, 122.60, 122.29, 120.43, 104.65, 70.46, 70.15, 69.79, 68.32, 67.72, 67.40, 58.72, 38.90, 3.67 ppm. LRMS found m/z = 482.22 $[M + H]^+$. HRMS expected m/z = 482.2192 for $[M + H]^+$, found m/z = 482.2202. UV-vis. (MeCN) λ_{max} (ε/dm^3 mol^{-1} cm^{-1}): 434 (9300), 280 (19 600), 262 (20 400) nm.

Synthesis of L^2. Prepared as for L^1, but using N^2 (0.10 g, 0.32 mmol), 2-pyridine carboxaldehyde (0.06 mL, 0.64 mmol), and sodium trisacetoxyborohydride (0.203 g, 0.13 mmol). Recrystallization from chloroform yielded the product as a yellow crystalline solid (0.08 g, 51%). ^{1}H NMR (400 MHz, $CDCl_3$): δ_H 8.83 (d, J = 8.2 Hz, 1H), 8.64 (d, J = 7.7 Hz, 1H), 8.59–8.56 (m, 2H), 8.42 (d, J = 8.6 Hz, 1H), 7.91 (s, 1H), 7.73–7.67 (m, 2H), 7.60–7.52 (m, 2H), 7.40–7.36 (m, 2H), 7.18–7.13 (m, 2H), 6.55 (d, J = 8.7 Hz, 1H), 4.44 (t, J = 6.0 Hz, 2H), 4.22 (t, J = 5.9 Hz, 2H), 4.01 (s, 4H), 3.73 (t, J = 6.3 Hz, 2H), 3.40 (s, 3H), 3.05 (t, J = 5.2 Hz, 2H) ppm. $^{13}C\{^1H\}$ NMR (101 MHz, CD_3OD): δ_C 153.26, 150.32, 147.84, 134.27, 131.02, 129.74, 128.47, 127.97, 124.60, 122.14, 120.86, 118.93, 109.67, 103.90, 69.27, 57.54, 48.94, 40.24, 39.01, 38.77, 38.45, 37.74, 36.45, 22.65, 13.02, 10.02 ppm. LRMS found m/z = 512.23 for $[M + O + H]^+$. HRMS expected m/z = 512.2281 for $[M + O + H]^+$, found m/z = 512.2292. UV-vis. (MeCN) λ_{max} (ε/dm^3 mol^{-1} cm^{-1}): 436 (10 420), 280 (19 800), 262 (20 500) nm.

Synthesis of L^3. Prepared as for L^1 but using N^3 (0.21 g, 0.565 mmol), 2-pyridine carboxaldehyde (0.13 mL, 1.12 mmol) and sodium trisacetoxyborohydride (0.36 g, 1.68 mmol). Product was isolated as an orange oil (0.386 g, 95%). ^{1}H NMR (400 MHz, $CDCl_3$): δ_H 8.48 (d, J = 4.7 Hz, 1H), 8.28 (d, J = 7.2 Hz, 1H), 8.18 (d, J = 8.4 Hz, 1H), 8.02 (d, J = 8.4 Hz, 1H), 7.59 (t, J = 7.6 Hz, 1H), 7.47 (d, J = 7.8 Hz, 1H), 7.35 (t, J = 7.8 Hz, 1H), 7.11–7.06 (m, 1H), 6.42 (d, J = 8.5 Hz, 1H), 5.91 (s, 1H), 4.36 (t, J = 4.1 Hz, 1H), 3.96 (t, J = 4.6 Hz, 1H), 3.76 (s, 2H), 3.23 (t, J = 5.6 Hz, 1H), 2.48 (t, J = 7.1 Hz, 1H), 1.70–1.64 (m, 1H), 1.53–1.48 (m, 1H), 1.37–1.25 (m, 2H) ppm. $^{13}C\{^1H\}$ NMR (101 MHz, $CDCl_3$): δ_C 164.25, 163.88, 158.88, 149.05, 147.87, 147.50, 135.65, 135.43, 133.59, 130.08, 128.52, 125.53, 123.30, 121.96, 121.26, 121.22, 120.95, 119.47, 118.98, 107.92, 103.03, 63.29, 60.72, 59.38, 53.17, 42.49, 41.50, 27.55, 25.90, 25.87, 25.66 ppm. LRMS found $m|z$ = 554.28 for $[M + O + H]^+$. HRMS expected m/z = 554.2753 for $[M + O + H]^+$, found m/z = 554.2762. UV-vis. (MeCN) λ_{max} (ε/dm^3 mol^{-1} cm^{-1}): 433 (7300), 279 (18 200, sh), 263 (20 400) nm.

Synthesis of L^4. Prepared as for L^1 but using N^4 (0.20 g, 0.51 mmol), 2-pyridine carboxaldehyde (0.1 mL, 1.08 mmol) and sodium trisacetoxyborohydride (0.34 g, 1.62 mmol). Product isolated as an orange oil (0.194 g, 69%).^{1}H NMR (400 MHz, $CDCl_3$) δ 8.56–8.49 (m, 3H), 8.43 (d, J = 7.7 Hz, 1H), 8.07 (d, J = 8.6 Hz, 1H), 7.63 (t, J = 7.7 Hz, 2H), 7.59–7.49 (m, 3H), 7.16–7.09 (app. t, J = 6.4 Hz, 2H), 6.66 (d, J = 8.3 Hz, 1H), 5.37 (s, 1H), 4.42 (t, J = 5.8 Hz, 2H), 3.81 (s, 4H), 3.42–3.32 (m, 5H), 2.56 (t, J = 7.1 Hz, 2H), 1.96–1.67 (m, 4H), 1.66–1.52 (m, 2H), 1.52–1.29 (m, 2H). $^{13}C\{^1H\}$ NMR (75 MHz, $CDCl_3$): δ_C 164.83, 164.20, 159.79, 149.76, 148.91, 136.50, 134.58, 131.16, 129.76, 126.28, 124.46, 122.98, 122.71, 122.02, 120.11, 109.54, 104.13, 77.53, 77.10, 76.68, 69.85, 60.40, 58.76, 54.21, 43.54, 38.91, 28.68, 26.92, 26.76 ppm. LRMS found m/z = 552.29 for $[M + H]^+$. HRMS expected m/z = 552.2955 for $[M + H]^+$, found m/z = 552.2969. UV-vis. (MeCN) λ_{max} (ε/dm^3 mol^{-1} cm^{-1}): 429 (8000), 282 (14 200, sh), 263 (17 500) nm.

Synthesis of L^5. N^5 (0.075 g, 0.19 mmol) was dissolved in 5% triethylamine in 1,2-dichloroethane and (20 mL) and 2-pyridinecarboxaldehyde (0.07 mL, 0.74 mmol) was added and the solution stirred for 2 hours under a nitrogen atmosphere. Sodium trisacetoxyborohydride (0.24 g, 1.11 mmol) was then added and the solution stirred at room temperature for 18 hours. The solution was then neutralised with saturated $NaHCO_3$ and the product extracted into chloroform, washed with water (3 × 20 mL) and brine (3 × 20 mL). The organic layer was then dried over $MgSO_4$ and filtered, and the solvent removed yielding L^5 as an orange oil (0.13 g, 73%). ^{1}H NMR (400 MHz, $CDCl_3$): δ_H 8.80 (d, J = 8.9 Hz, 1H), 8.57 (d, J = 7.3 Hz, 1H), 8.52–8.49 (m, 2H), 8.35 (d, J = 8.6 Hz, 1H), 7.98 (s, 1H), 7.68–7.60 (m, 1H), 7.55–7.47 (m, 2H), 7.31 (d, J = 7.6 Hz, 2H), 7.12–7.07 (m, 2H), 6.48 (d, J = 8.1 Hz, 1H), 4.70 (s, 1H), 4.43–4.38 (m, 2H), 3.95 (s, 4H), 3.93–3.89 (m, 2H), 3.36–3.31 (m, 2H), 3.01–2.96 (m, 2H) ppm. $^{13}C\{^1H\}$ NMR (75 MHz, $CDCl_3$): δ_C 165.52, 165.05, 159.26, 150.55, 148.88, 136.61, 134.76, 131.23, 129.77, 127.74, 124.27, 123.24, 122.13, 120.49, 109.09, 103.98, 77.52, 77.09, 76.67, 70.29, 69.25, 68.64, 61.91, 60.60, 53.83, 43.35, 42.60 ppm. LRMS found m/z = 570.27 for $[M + H]^+$. HRMS expected m/z = 570.2711 for $[M + H]^+$, found m/z = 570.2708. UV-vis. (MeCN) λ_{max} (ε/dm^3 mol^{-1} cm^{-1}): 429 (8190), 279 (19 200, sh), 260 (21 000) nm.

Synthesis of L^6. Prepared as for L^5 but using N^6 (0.06 g, 0.15 mmol), 2-pyridine carboxaldehyde (0.03 g, 0.3 mmol) and sodium trisacetoxyborohydride (0.1 g, 0.45 mmol) and triethylamine (2 mL). L^2 was isolated as a red oil (0.063 g, 72%). ^{1}H NMR (500 MHz, $CDCl_3$): δ_H 8.47 (d, J = 7.3 Hz, 1H), 8.42 (d, J = 4.3 Hz, 2H), 8.38 (d, J = 8.4 Hz, 1H), 8.17 (d, J = 7.9 Hz, 1H), 7.53 (t, J = 7.1 Hz, 2H), 7.45–7.38 (m, 3H), 7.06–7.02 (m, 2H), 6.60 (d, J = 8.5 Hz, 1H), 6.24 (s, 1H), 4.35 (t, J = 6.0 Hz, 2H), 3.87 (s, 4H), 3.79 (t, J = 4.7 Hz, 2H), 3.66 (t, J = 6.0 Hz, 2H), 3.61 (d, J = 4.8 Hz, 4H), 3.55–3.52 (m, 2H), 3.48 (d, J = 4.8 Hz, 2H) ppm. $^{13}C\{^1H\}$ NMR (126 MHz, $CDCl_3$): δ_C 165.02, 164.38, 159.72, 150.04, 149.12, 136.60, 134.74, 131.39, 130.10, 127.08, 124.66, 123.08, 122.95, 122.47, 122.15, 120.74, 110.21, 104.34, 70.48, 70.35, 69.95, 69.67, 68.71, 60.87, 58.92, 53.66, 43.28, 39.08. LRMS found m/z = 584.28 $[M + H]^+$. HRMS expected m/z = 584.2867 for $[M + H]^+$, found m/z = 584.2873. UV-vis. (MeCN) λ_{max} (ε/dm^3 mol^{-1} cm^{-1}): 429 (7920), 281 (19 600), 263 (20 600) nm.

Synthesis of *fac*-[Re(CO)$_3$(L^1)]BF_4. Compound L^1 (50 mg, 0.10 mmol) was dissolved in chloroform and *fac*-[Re(CO)$_3$(MeCN)$_3$]BF_4 (54 mg, 0.11 mmol) was added and the solution stirred at reflux under a nitrogen atmosphere for 18 h. Upon being allowed to cool, the solvent was reduced to a minimum and the product precipitated upon the dropwise addition of hexane. The product was then filtered to yield *fac*-[Re(CO)$_3$(L^1)]BF_4 as an orange solid (21.5 mg, 35%). ^{1}H NMR (300 MHz, CD_3CN): δ_H 8.78 (d, J = 5.3 Hz, 2H), 8.54 (d, J = 7.5 Hz, 1H), 8.44 (dd, J = 8.3, 5.4 Hz, 2H), 7.89 (t, J = 7.7 Hz, 2H), 7.77–7.69 (m, 1H), 7.49–7.41 (m, 2H), 7.35–7.27 (m, 2fH), 6.95 (d, J = 8.5 Hz, 1H), 6.40 (s, 1H), 5.01–4.81 (m, 4H), 4.22 (dd, J = 12.3, 6.4 Hz, 2H), 4.03–3.92 (m, 2H), 3.74 (t, J = 6.2 Hz, 2H) ppm. $^{13}C\{^1H\}$ NMR (151 MHz, d_6-DMSO): δ_C 196.90, 195.60, 164.33, 163.59, 160.98, 152.34, 152.29, 150.52, 141.21, 141.20, 141.15, 134.51, 131.30, 129.79, 129.02, 126.29, 125.18, 123.85, 122.64, 120.89, 109.47, 104.79, 67.77, 67.68, 67.42, 58.45,

58.41, 41.93. LRMS found m/z = 752.15 for $[M]^+$. HRMS expected m/z = 752.1506 for $[M]^+$, found m/z = 752.1515. FT-IR (solid, selected cm^{-1}): 2027 (C≡O), 1904 (C≡O), 1684 (C═O), 1638 (C═O), 1057 (BF_4^-). UV-vis. (MeCN) λ_{max} (ε/dm^3 mol^{-1} cm^{-1}): 430 (8560), 281 (18 900, sh), (21 000) nm.

Synthesis of *fac*-[Re(CO)$_3$(L^2)]BF$_4$. Prepared as for *fac*-[Re(CO)$_3$(**L**^{1})]BF_4 but using compound **L**^{2} (58 mg, 1.0 mmol). ^{1}H NMR (400 MHz, $CDCl_3$): δ_H 8.68 (d, J = 8.0 Hz, 1H), 8.64 (d, J = 5.3 Hz, 2H), 8.59 (d, J = 7.3 Hz, 1H), 8.48 (d, J = 8.2 Hz, 1H), 7.81–7.66 (m, 5H), 7.22–7.17 (m, 2H), 6.73 (d, J = 8.5 Hz, 1H), 5.80 (d, J = 16.0 Hz, 2H), 4.52 (d, J = 16.0 Hz, 2H), 4.41 (t, J = 5.8 Hz, 2H), 4.28–4.15 (m, 4H), 3.71 (t, J = 6.7 Hz, 2H), 3.37 (s, 3H) ppm. $^{13}C\{^1H\}$ NMR (151 MHz, $CDCl_3$): δ_C 195.74, 195.73, 164.76, 164.11, 160.85, 150.59, 150.53, 140.25, 134.54, 131.29, 129.82, 127.09, 125.21, 125.00, 124.53, 122.60, 122.29, 120.43, 70.46, 70.46, 70.15, 69.79, 68.32, 67.72, 67.40, 58.72, 43.70, 38.90 ppm. LRMS found m/z = 766.17 for $[M]^+$. HRMS expected m/z = 766.1657 for $[M^+]$, found m/z 766.1671. FT-IR (solid, selected cm^{-1}): 2029 (C≡O), 1910 (C≡O), 1684 (C═O), 1638 (C═O), 1055 (BF_4^-). UV-vis. (MeCN) λ_{max} (ε/dm^3 mol^{-1} cm^{-1}): 433 (9800), 280 (18 400, sh), 261 (22 500) nm.

Synthesis of *fac*-[Re(CO)$_3$(L^3)]BF$_4$. Prepared as for *fac*-[Re(CO)$_3$(**L**^{1})]BF_4 but using compound **L**^{3} (58 mg, 1.0 mmol). ^{1}H NMR (400 MHz, $CDCl_3$): δ_H 8.68 (d, J = 8.0 Hz, 1H), 8.64 (d, J = 5.3 Hz, 2H), 8.59 (d, J = 7.3 Hz, 1H), 8.48 (d, J = 8.2 Hz, 1H), 7.81–7.66 (m, 5H), 7.22–7.17 (m, 2H), 6.73 (d, J = 8.5 Hz, 1H), 5.80 (d, J = 16.0 Hz, 2H), 4.52 (d, J = 16.0 Hz, 2H), 4.41 (t, J = 5.8 Hz, 2H), 4.28–4.15 (m, 4H), 3.71 (t, J = 6.7 Hz, 2H), 3.37 (s, 3H) ppm. $^{13}C\{^1H\}$ NMR (151 MHz, CD_3OD): δ_C 197.13, 196.19, 166.18, 165.72, 161.91, 161.34, 153.23, 151.64, 141.75, 135.67, 132.45, 131.10, 129.28, 127.20, 127.02, 126.08, 124.81, 124.73, 110.94, 105.56, 70.70, 68.94, 68.91, 58.94, 49.85, 40.47, 39.88 ppm. LRMS found m/z = 808.21 for $[M]^+$. HRMS expected m/z = 808.2137 for $[M]^+$, found m/z = 808.2140. FT-IR (solid, selected cm^{-1}): 2031 (C≡O), 1944 (C≡O), 1638 (C═O), 1072 (BF_4^-). UV-vis. (MeCN) λ_{max} (ε/dm^3 mol^{-1} cm^{-1}): 434 (10 100), 279 (18 200), 256 (22 400) nm.

Synthesis of *fac*-[Re(CO)$_3$(L^4)]BF$_4$. Prepared as for *fac*-[Re(CO)$_3$(**L**^{1})]BF_4 but using compound **L**^{4} (62 mg, 1.0 mmol). ^{1}H NMR (400 MHz, $CDCl_3$): δ_H 8.66–8.54 (m, 3H), 8.52 (d, J = 7.2 Hz, 1H), 8.41 (d, J = 8.3 Hz, 1H), 7.71 (app. t, J = 7.9 Hz, 2H), 7.63 (app. t, J = 10.7 Hz, 3H), 7.15–7.10 (m, 3H), 5.73 (d, J = 16.0 Hz, 2H), 4.45 (d, J = 16.0 Hz, 2H), 4.34 (t, J = 6.3 Hz, 2H), 4.21–4.08 (m, 4H), 3.64 (t, J = 6.4 Hz, 2H), 3.31 (s, 3H), 1.14 (t, J = 7.1 Hz, 4H) ppm. $^{13}C\{^1H\}$ NMR (151 MHz, CD_3OD): δ_C 195.52, 195.30, 164.77, 164.25, 160.51, 159.92, 151.82, 150.21, 140.52, 140.34, 134.40, 130.92, 128.80, 127.73, 125.62, 125.43, 124.61, 123.40, 123.32, 109.53, 104.15, 69.29, 67.53, 67.50, 57.54, 48.47, 48.20, 48.10, 47.17, 46.56, 39.06, 38.48 ppm. LRMS found m/z = 822.23 for $[M]^+$. HRMS expected m/z = 822.2301 for $[M]^+$, found m/z = 822.2290 for $[M]^+$. FT-IR (solid, selected cm^{-1}): 2029 (C≡O), 1907 (C≡O), 1681 (C═O), 1639 (C═O), 1055 (BF_4^-). UV-vis. (MeCN) λ_{max} (ε/dm^3 mol^{-1} cm^{-1}): 431 (13 020), 276 (24 400, sh), 260 (26 100) nm.

Synthesis of *fac*-[Re(CO)$_3$(L^5)]BF$_4$. Prepared as for *fac*-[Re(CO)$_3$(**L**^{1})]BF_4 but using compound **L**^{5} (62 mg, 0.10 mmol). ^{1}H NMR (300 MHz, $CDCl_3$): δ_H 8.54 (d, J = 5.0 Hz, 2H), 8.47 (d, J = 7.4 Hz, 1H), 8.41 (d, J = 8.4 Hz, 2H), 7.62–7.46 (m, 5H), 7.12 (t, J = 6.4 Hz, 2H), 6.73 (d, J = 7.6 Hz, H), 5.22 (d, J = 17.0 Hz, 2H), 4.48–4.37 (m, 4H), 4.01–3.90 (m, 8H), 3.84 (s, 4H), 3.66 (t, J = 5.1 Hz, 2H) ppm. $^{13}C\{^1H\}$ NMR (151 MHz, $CDCl_3$): δ_C 195.75, 195.36, 165.59, 165.12, 160.83, 150.51, 140.00, 134.96, 131.50, 129.88, 127.58, 125.25, 124.96, 124.50, 122.30, 120.33, 109.29, 104.33, 77.23, 77.02, 76.81, 70.45, 70.13, 68.39, 67.71, 67.41, 62.49, 43.29, 42.71 ppm. LRMS found m/z = 840.20 $[M + H]^+$, HRMS expected m/z = 840.2043 for $[M + H]^+$, found m/z = 840.2029. FT-IR (solid, selected cm^{-1}): 2031 (C≡O), 1928 (C≡O), 1683 (C═O), 1635 (C═O), 1058 (BF_4^-). UV-vis. (MeCN) λ_{max} (ε/dm^3 mol^{-1} cm^{-1}): 429 (8100), 279 (13 300), 262 (18 000) nm.

Synthesis of *fac*-[Re(CO)$_3$(L^6)]BF$_4$. Prepared as for *fac*-[Re(CO)$_3$(**L**^{5})]BF_4 but using compound **L**^{6} (62 mg, 1.0 mmol). ^{1}H NMR (300 MHz, $CDCl_3$): δ_H 8.54 (d, J = 4.9 Hz, 2H), 8.50–8.34 (m, 3H), 7.62–7.46 (m, 5H), 7.11 (app. t, J = 5.7 Hz, 2H), 6.73 (d, J = 8.4 Hz, 1H), 5.23 (d, J = 16.6 Hz, 2H), 4.46 (s, 1H), 4.40 (t, J = 6.3 Hz, 3H), 4.03–3.91 (m, 5H), 3.85 (s, 4H), 3.72 (t, J = 6.1 Hz, 3H), 3.69–3.63 (m, 2H), 3.39 (s, 3H) ppm. $^{13}C\{^1H\}$ NMR (151 MHz, CD_3OD): δ_C 195.81, 194.75, 164.73, 164.19, 160.54, 151.54, 151.12, 139.90, 134.49, 130.83, 129.85, 127.58, 125.12, 124.34, 122.95, 122.07, 120.19, 108.16, 103.83, 70.22, 70.10, 69.35, 69.27, 68.63, 68.04, 67.77, 57.48, 42.96, 38.36 ppm. LRMS found m/z = 854.21 $[M]^+$, HRMS expected m/z = 854.2196 for $[M]^+$, found m/z = 854.2190. FT-IR (solid, selected cm^{-1}): 2029 (C≡O), 1908 (C≡O), 1684 (C═O), 1645 (C═O), 1057 (BF_4^-). UV-vis. (MeCN) λ_{max} (ε/dm^3 mol^{-1} cm^{-1}): 430 (12 240), 281 (21 000), 261 (23 100) nm.

Conflicts of interest

There are no conflicts to declare.

Acknowledgements

AD, IAF and SJAP thank DSTL and Ministry of Defence for financial support. The staff of the EPSRC Mass Spectrometry National Service (Swansea University) are also thanked. We also thank EPSRC for instrumentation grant EP/L027240/1. We acknowledge the Daisy Appeal Charity (grant no. DAhul2011) for funding, and thank Dr Assem Allam and his family for the generous donation to help found the PET Research Centre at the University of Hull.

Notes and references

1 B. P. Burke, C. Cawthorne and S. J. Archibald, *Philos. Trans. R. Soc., A*, 2017, **375**, 0261.
2 S. Lutje, M. Rijpkema, W. Helfrich, W. J. G. Oyen and O. C. Boerman, *Mol. Imaging Biol.*, 2014, **16**, 747–755.
3 (*a*) L. E. Jennings and N. J. Long, *Chem. Commun.*, 2009, **28**, 3511–3524; (*b*) S. Lee and X. Chen, *Mol. Imaging*, 2009, **8**,

87–100; (*c*) S. R. Cherry, *Annu. Rev. Biomed. Eng.*, 2006, **8**, 35–62; (*d*) X. Li, X.-N. Zhang, X.-D. Li and J. Chang, *Cancer Biol. Med.*, 2016, **13**, 339–348; (*e*) F. L. Thorp-Greenwood and M. P. Coogan, *Dalton Trans.*, 2011, **40**, 6129–6143.

4 A. Azhdarinia, P. Ghosh, S. Ghosh, N. Wilganowski and E. M. Sevick-Muraca, *Mol. Imaging Biol.*, 2012, **14**, 261–276.

5 D. L. Li, J. J. Zhang, C. W. Chi, X. Xiao, J. M. Wang, L. X. Lang, I. Ali, G. Niu, L. W. Zhang, J. Tian, N. Ji, Z. H. Zhu and X. Y. Chen, *Theranostics*, 2018, **8**, 2508–2520.

6 E. Mery, M. Golzio, S. Guillermet, D. Lanore, A. Le Naour, B. Thibault, A. F. Tilkin-Mariame, E. Bellard, J. P. Delord, D. Querleu, G. Ferron and B. Couderc, *Oncotarget*, 2017, **8**, 109559–109574.

7 A. L. Vahrmeijer, M. Hutteman, J. R. van der Vorst, C. J. H. van de Velde and J. V. Frangioni, *Nat. Rev. Clin. Oncol.*, 2013, **10**, 507–518.

8 (*a*) A. Mahmood and A. G. Jones, Technetium Radiopharmaceuticals, in *Handbook of Radiopharmaceuticals*, ed. M. J. Welch and C. S. Redvanly, Wiley, 2005, ch. 10; (*b*) P. J. Blower, *Dalton Trans.*, 2015, **44**, 4819–4844.

9 (*a*) M. H. Kim, C. G. Kim, S.-G. Kim and D.-W. Kim, *J. Labelled Compd. Radiopharm.*, 2017, **60**, 649–658; (*b*) M. H. Kim, S.-G. Kim and D.-W. Kim, *J. Labelled Compd. Radiopharm.*, 2018, **61**, 557–566; (*c*) J. Y. Lee, H. J. Kim, Y.-S. Lee and J. M. Jeong, *Sci. Rep.*, 2018, **8**, 13636; (*d*) M. Stalnionis and R. Rotomskis, *Phys. Med.*, 2014, **30**, e120.

10 M. P. Coogan, R. P. Doyle, J. F. Valliant, J. W. Babich and J. Zubieta, *J. Labelled Compd. Radiopharm.*, 2014, **57**, 255–261.

11 (*a*) V. Fernandez-Moreira, F. L. Thorp-Greenwood and M. P. Coogan, *Chem. Commun.*, 2010, **46**, 186–202.

12 M. Sagnou, B. Mavroidi, A. Shegani, M. Paravatou-Petsotas, C. Raptopoulou, V. Psycharis, I. Permettis, M. S. Papadopoulos and M. Pelecanou, *J. Med. Chem.*, 2019, **62**, 2638–2650.

13 T. Storr, K. H. Thompson and C. Orvig, *Chem. Soc. Rev.*, 2006, **35**, 534–544.

14 For example: (*a*) D. J. Hayne, A. J. North, M. Fodero-Tavoletti, J. M. White, L. W. Hung, A. Rigopoulos, C. A. McLean, P. A. Adlard, U. Ackermann, H. Tochon-Danguy, V. L. Villemagne, K. J. Barnham and P. S. Donnelly, *Dalton Trans.*, 2015, **44**, 4933–4944; (*b*) C. Xiong, W. Lu, R. Zhang, M. Tian, W. Tong, J. Gelovani and C. Li, *Chem. – Eur. J.*, 2009, **15**, 8979–8984.

15 E. B. Bauer, A. A. Haase, R. M. Reich, D. C. Crans and F. E. Kuhn, *Coord. Chem. Rev.*, 2019, **393**, 79–117.

16 (*a*) S. Jurgens, W. A. Herrmann and F. E. Kuhn, *J. Organomet. Chem.*, 2014, **751**, 83–89; (*b*) P. S. Donnelly, *Dalton Trans.*, 2011, **40**, 999–1010; (*c*) B. Lambert, K. Bacher and L. Defreyne, *J. Nucl. Med. Mol. Imaging*, 2009, **53**, 305–310.

17 F.-X. Wang, J.-H. Liang, H. Zhang, Z.-H. Wang, Q. Wan, C.-P. Tan, L.-N. Ji and Z.-W. Mao, *ACS Appl. Mater. Interfaces*, 2019, **11**, 13123–13133.

18 A. François, C. Auzanneau, V. Le Morvan, C. Galaup, H. S. Godfrey, L. Marty, A. Boulay, M. Artigau, B. Mestre-Voegtlé, N. Leygue, C. Picard, Y. Coulais, J. Robert and E. Benoist, *Dalton Trans.*, 2014, **43**, 439.

19 For example: (*a*) L. Wei, J. W. Babich, W. Oullette and J. Zubieta, *Inorg. Chem.*, 2006, **45**, 3057–3066; (*b*) N. Agorastos, L. Borsig, A. Renard, P. Antoni, G. Viola, B. Springler, P. Kurz and R. Alberto, *Chem. – Eur. J.*, 2007, **13**, 3842–3853; (*c*) P. Haefliger, N. Agorastos, A. Renard, G. Giambonini-Brugnoli, C. Marty and R. Alberto, *Bioconjugate Chem.*, 2005, **16**, 582–587; (*d*) E. E. Langdon-Jones, A. B. Jones, C. F. Williams, A. J. Hayes, D. Lloyd, H. J. Mottram and S. J. A. Pope, *Eur. J. Inorg. Chem.*, 2016, 759–766.

20 F. J. Dai, H. Y. He, X. J. Xu, S. Chen, C. J. Wang, C. Y. Feng, Z. Y. Tian, H. Y. Dong and S. Q. Xie, *Bioorg. Chem.*, 2018, **77**, 16–24.

21 E. Calatrava-Perez, S. A. Bright, S. Achermann, C. Moylan, M. O. Senge, E. B. Veale, D. C. Williams, T. Gunnlaugsson and E. M. Scanlan, *Chem. Commun.*, 2016, **52**, 13086–13089.

22 E. E. Langdon-Jones, C. F. Williams, A. J. Hayes, D. Lloyd, S. J. Coles, P. N. Horton, L. M. Groves and S. J. A. Pope, *Eur. J. Inorg. Chem.*, 2017, 5279–5287.

23 C. Satriano, G. T. Sfrazzetto, M. E. Amato, F. P. Ballistreri, A. Copani, M. L. Giuffrida, G. Grasso, A. Pappalardo, E. Rizzarelli, G. A. Tomaselli and R. M. Toscano, *Chem. Commun.*, 2013, **49**, 5565–5567.

24 E. E. Langdon-Jones, D. Lloyd, A. J. Hayes, S. D. Wainwright, H. J. Mottram, S. J. Coles, P. N. Horton and S. J. A. Pope, *Inorg. Chem.*, 2015, **54**, 6606–6615.

25 S. Nigam, B. P. Burke, L. H. Davies, J. Domarkas, J. F. Wallis, P. G. Waddell, J. S. Waby, D. M. Benoit, A. M. Seymour, C. Cawthorne, L. J. Higham and S. J. Archibald, *Chem. Commun.*, 2016, **52**, 7114–7117.

26 W. L. Turnbull, E. Murrell, M. Bulcan-Gnirss, M. Majeed, M. Milne and L. G. Luyt, *Dalton Trans.*, 2019, **48**, 14077–14084.

27 T. Storr, Y. Sugai, C. A. Barta, M. J. Adam, S. Yano and C. Orvig, *Inorg. Chem.*, 2005, **44**, 2698–2705.

28 J. A. Czaplewska, F. Theil, E. Altuntas, T. Niksch, M. Freesmeyer, B. Happ, D. Pretzel, H. Schafer, M. Obata, S. Yano, U. S. Schubert and M. Gottschaldt, *Eur. J. Inorg. Chem.*, 2014, 6290–6297.

29 L. A. Mullice, R. H. Laye, L. P. Harding, N. J. Buurma and S. J. A. Pope, *New J. Chem.*, 2008, **32**, 2140–2149.

30 R. M. Duke, E. B. Veale, F. M. Pfeffer, P. E. Kruger and T. Gunnlaugsson, *Chem. Soc. Rev.*, 2010, **39**, 3936–3953.

31 E. E. Langdon-Jones, N. O. Symonds, S. E. Yates, A. J. Hayes, D. Lloyd, R. Williams, S. J. Coles, P. N. Horton and S. J. A. Pope, *Inorg. Chem.*, 2014, **53**, 3788–3797.

32 R. Alberto, *J. Organomet. Chem.*, 2007, **692**, 1179–1186.

33 R. Alberto, R. Schibli, A. Egli, A. P. Schubiger, U. Abram and T. A. Kaden, *J. Am. Chem. Soc.*, 1998, **120**, 7987–7988.

34 B. B. Kasten, X. Ma, K. Cheng, L. Bu, W. S. Slocumb, T. R. Hayes, S. Trabue, Z. Cheng and P. D. Benny, *Bioconjugate Chem.*, 2016, **27**, 130–142.
35 A. J. Hallett, E. Placet, R. Prieux, D. McCafferty, J. A. Platts, D. Lloyd, M. Isaacs, A. J. Hayes, S. J. Coles, M. B. Pitak, S. Marchant, S. N. Marriott, R. K. Allemann, A. Dervisi and I. A. Fallis, *Dalton Trans.*, 2018, **47**, 14241–14253.
36 L. Di and E. H. Kerns, *Curr. Opin. Chem. Biol.*, 2003, **7**, 402–408.
37 J. E. A. Comer, High throughput measurement of logD and pKa, in *Methods and Principlesin Medicinal Chemistry*, ed. P. Artursson, H. Lennernas and H. van de Waterbeemd, Wiley-VCH, Weinheim, 2003, vol. 18, p. 21.
38 C. Moura, F. Mendes, L. Gano, I. Santos and A. Paulo, *J. Inorg. Biochem.*, 2013, **123**, 34–45.
39 R. A. Fearn and B. H. Hirst, *Environ. Toxicol. Pharmacol.*, 2006, **21**, 168.
40 W. L. Turnbull, L. Yu, E. Murrell, M. Milne, C. L. Charron and L. G. Luyt, *Org. Biomol. Chem.*, 2019, **17**, 598.
41 P. Workman, E. O. Aboagye, F. Balkwill, A. Balmain, G. Bruder, D. J. Chaplin, J. A. Double, J. Everitt, D. A. H. Farningham, M. J. Glennie, L. R. Kelland, V. Robinson, I. J. Stratford, G. M. Tozer, S. Watson, S. R. Wedge, S. A. Eccles, V. Navaratnam, S. Ryder and Committe of the National Cancer Research Institute, *Br. J. Cancer*, 2010, **102**, 1555.
42 E. A. Boehm, B. E. Jones, G. K. Radda, R. L. Veech and K. Clarke, *Am. J. Physiol.: Heart Circ. Physiol.*, 2001, **280**, 977.
43 K. Sakayori, Y. Shibasaki and M. Ueda, *J. Polym. Sci., Part A: Polym. Chem.*, 2005, **43**, 5571.
44 X. Chen, C. Xu, T. Wang, C. Zhou, J. Du, Z. Wang, H. Xu, T. Xie, G. Bi, J. Jiang, X. Zhang, J. N. Demas, C. O. Trindle, Y. Luo and G. Zhang, *Angew. Chem., Int. Ed.*, 2016, **55**, 9872–9876.